Supplementary Text

Composition and Mineralogy of Chondrule Fragments in OREX-803417-103

Particle OREX-803417-103, ~ 1.5 mm in length, has a pseudo-rectangular morphology and an irregular surface texture (Fig. 5a). FESEM imaging of the particle's topside and underside reveals a total of 25 fragments (23 on the upper particle surface and 2 on the underside (not shown)) composed primarily of Mg-rich olivine and infrequent Mg-rich, low-Ca pyroxene. These silicate grains are elongated with rounded edges and perforated textures separated by void space. Two of the largest regions, shown at higher magnification in Fig. 5b-e, contain silicate grains ranging in width from <1 to 3 μm. These grains consist primarily of nearly pure Mg-rich olivine (average Mg# 97) and low-Ca, Mg-rich pyroxene (average Mg# 97) (see Extended Data Table 5 and Supplementary Data Table 5). No mesostasis or replacement phyllosilicates were detected within the pore spaces, although rare occurrences of a Mg-bearing phase compositionally similar to those observed in OREX-803437-100 (Extended Data Table 2) and OREX-803079-241 (Extended Data Table 4) are present.

XCT analysis of particle OREX-803417-103 identified ~ 18 internal barred fragments, with two of the largest ranging from ~ 100 to 180 μm in size, having surfaces that partially breach the exterior surface of the particle (Fig. 5a-e; Supplementary Data Video 3).

Composition and Mineralogy of Chondrule Fragment in OREX-803429-100

Particle OREX-803429-100, ~ 0.65 mm in length, has an elongated triangular morphology and an irregular surface texture (Fig. 5f). Optical imaging (Fig. 5f, inset) and magnified FESEM imaging (Fig. 5g) reveal a single chondrule fragment composed of Fe-bearing olivine (average Mg# 73), and low-Ca, Fe-bearing pyroxene (average Mg# 76) (Extended Data Table 5 and Supplementary Data Table 5). The elongated silicate grains have rounded edges and are separated by void space. No mesostasis or replacement phyllosilicates were detected.

On the Nature of the Fluid After Mesostasis Dissolution

The composition of the fluid that dissolved chondrule mesostasis can be approximated from the chemistry of that mesostasis itself. Semarkona (LL3.0) chondrules provide the best available analog for this purpose because they are among the least thermally and aqueously altered

materials in meteorite collections. Their primary glassy mesostasis is well preserved and has been chemically characterized at high spatial resolution, offering a robust reference for the unmodified composition of chondrule melts prior to secondary processing[52]. Although Semarkona belongs to the ordinary chondrite rather than the carbonaceous chondrite clan, its chondrules broadly share similar silicate mineralogy, cooling histories, and melt chemistry with type I chondrules in primitive carbonaceous meteorites.

In Semarkona chondrules, mesostasis glass is dominantly Al-Si–rich with substantial Ca and measurable alkalis[52] (typically 0.1–4 wt% Na_2O and 0–0.2 wt% K_2O). It also contains minor P, Cl, Ti, and Cr, and shows pronounced enrichments of Na, K, and Cl in outer zones where Ca is depleted. Dissolution of such a phase into an aqueous medium would have produced a Si- and Al-rich, mildly alkaline solution containing alkalis, halogens, and trace oxyanions. This inferred fluid composition — alkali-bearing, saline, and variably enriched in dissolved silica — suggests a mobile aqueous phase capable of reacting with other components of Bennu's parent body. Although its subsequent fate remains uncertain, such a fluid must have migrated beyond the immediate chondrule environment, contributing to redistribution of major and trace elements within Bennu's parent body. Finally, we note that the preservation of a well-organized barred and radial framework suggests that if mesostasis was present, its dissolution may have exploited pre-existing inter-crystalline cavities established during chondrule crystallization.

Isotopic Heterogeneity in Bennu Chondrule Fragments

The oxygen-isotopic compositions of olivine within Bennu chondrule fragments provide additional constraints on their origin and subsequent alteration (Fig. 6). The porphyritic olivine–pyroxene fragment in OREX-803437-100 plots along the PCM line and is consistent with an origin from a ^{16}O-rich reservoir typical of type I chondrules in CM and CR chondrites[43,53]. In contrast, the barred olivine fragment in OREX-803079-241, lying slightly above the PCM line, suggests partial equilibration with an isotopically heavier reservoir. This isotopic offset may reflect limited oxygen exchange with ^{18}O-enriched aqueous fluids during low-temperature alteration on Bennu or its progenitor body. The coexistence of both ^{16}O-rich and ^{16}O-poor chondrule fragments within Bennu indicates that materials derived from isotopically distinct nebular reservoirs were incorporated into a single parent body[8]. Such isotopic heterogeneity, combined with textural and

mineralogical evidence for variable aqueous processing, reinforces the interpretation that Bennu represents a complex accretionary aggregate of materials formed under diverse nebular and parent-body conditions.

Supporting Data for Tables and Figures

Supplementary Data 1. Figure and Table comparing results of EDX point spectra to Electron Microprobe spot analyses (Methods Section)

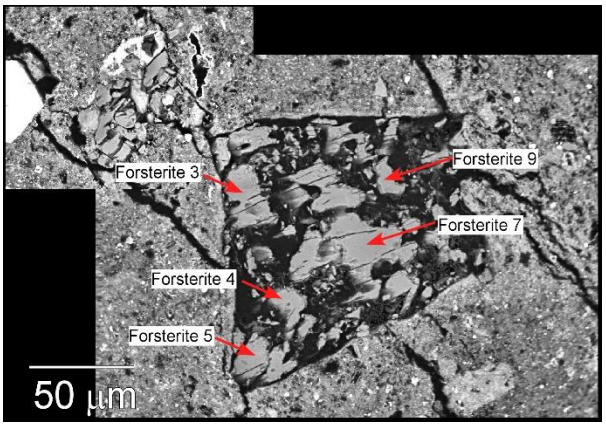

***Left view*:** FESEM LABE image of the internal polished chondrule fragment in OREX-803079-241 (also see Fig. 4) showing locations of point analyses acquired by EMPA and SEM-EDX.

***Lower view*:** Tabular results indicate EPMA-WDS and SEM-EDX analyses of the major and minor elements comprising chondrule olivine are comparable.

Element (Wt%)	O	Mg	Al	Si	Ca	Cr	Mn	Fe	Mg/Si (wt%)
Microprobe (15 kV 20 nA 60 s.)									
Forsterite 3	44.42	34.33	0.00	19.48	0.14	0.20	0.02	1.41	1.76
Forsterite 4	42.94	35.10	0.02	20.11	0.14	0.25	0.02	1.41	1.75
Forsterite 5	43.69	34.71	0.01	19.70	0.12	0.25	0.04	1.48	1.76
Forsterite 7	44.52	34.04	0.00	19.60	0.12	0.26	0.03	1.41	1.74
Forsterite 9	43.15	35.28	0.01	19.76	0.12	0.24	0.03	1.42	1.79
Ave ± STD	43.75 ± 0.72	34.69 ± 0.52	0.01 ± 0.01	19.73 ± 0.24	0.13 ± 0.01	0.24 ± 0.02	0.03 ± 0.01	1.43 ± 0.03	1.76
SEM-EDX (15 kV 1 nA 30 s. O by stoichiometry)									
Forsterite 3	44.87	33.73	0.04	19.31	0.11	0.25	0.04	1.65	1.75
Forsterite 4	44.92	33.66	0.05	19.40	0.13	0.27	0.02	1.55	1.74
Forsterite 5	44.88	33.69	0.07	19.30	0.13	0.32	0.03	1.58	1,75
Forsterite 7	44.94	33.76	0.05	19.39	0.12	0.29	0.07	1.38	1.74
Forsterite 9	44.94	33.84	0.07	19.33	0.14	0.23	0.07	1.38	1.75
Ave ± STD	44.90 ± 0.03	33.74 ± 0.07	0.06 ± 0.01	19.35 ± 0.05	0.13 ± 0.01	0.27 ± 0.04	0.05 ± 0.02	1.51 ± 0.12	1.74
Forsterite Standard (Mg_2SiO_4)	45.47	34.56	---	19.97	---	---	---	---	1.73

Supplementary Data for Table 2. SEM-EDX of Mineral Phases in OREX-803437-100 POP Chondrule Fragment

See file: Supplementary Data for Table 2.xlsx

Supplementary Data for Table 3. SEM-EDX of Mineral Phases in OREX-803079-241 Chondrule Fragments (upper surface)

See file: Supplementary Data for Table 3.xlsx

Supplementary Data for Table 4. SEM-EDX of Mineral Phases in OREX-803079-241 Chondrule Fragment (internal/polished)

See file: Supplementary Data for Table 4.xlsx

Supplementary Data for Table 5. SEM-EDX of Mineral Phases in OREX-803417-103 and OREX-803429-100 Chondrule Fragments

See file: Supplementary Data for Table 5

Supplementary Data Table for Figure 2a. Si/Mg vs. Fe/Mg for Bennu chondrules in comparison to select literature data

See file: Supplementary Data Table for Figure 2a.xlsx

Supplementary Data Table for Figure 6. $\delta^{18}O$ vs. $\delta^{17}O$ for Bennu chondrule olivine

See file: Supplementary Data Table for Figure 6.xlsx

92 ***Supplementary Data Table 7. Data and corresponding DOIs (Incomplete—TBD)***

Figure	*Sample Number*	*Technique*	*doi*
1a	OREX-803437-100	SEM	
1a-Inset image left	OREX-803437-100	SEM	
1a-Inset image right	OREX-803437-100	SEM	
1b	OREX-803437-100	SEM/EDX map overlay	
2a	OREX-803437-100; OREX-803079-241	SEM/EDX	
2b	OREX-803437-100; OREX-803079-241	SEM/EDX	
2c	OREX-803437-100; OREX-803079-241	SEM/EDX	
3a	OREX-803079-241	Optical	
3b	OREX-803079-241	SEM	
3b-Inset	OREX-803079-241	SEM	
3c	OREX-803079-241	SEM	
3c-Inset	OREX-803079-241	SEM	
4a	OREX-803079-241	SEM	
4b	OREX-803079-241	SEM	
4c	OREX-803079-241	SEM	
4d	OREX-803079-241	SEM	
4e	OREX-803079-241	SEM/EDX	
4f	OREX-803079-241	XCT reconstruction	
4g	OREX-803079-241	XCT reconstruction	
4h	OREX-803079-241	XCT reconstruction	

5a	OREX-803417-103	SEM
5b	OREX-803417-103	SEM
5c	OREX-803417-103	SEM
5d	OREX-803417-103	SEM
5e	OREX-803417-103	SEM
5f	OREX-803429-100	SEM
5f-Insert	OREX-803429-100	Optical
5g	OREX-803429-100	SEM
6	OREX-803437-100; OREX-803079-241	NanoSIMS
Extended Data Figures		
1a	OREX-803437-100	SEM
1b	OREX-803437-100	SEM
1c	OREX-803437-100	SEM
1d	OREX-803437-100	SEM
1e	OREX-803437-100	SEM/EDX
1f	OREX-803437-100	SEM/EDX
2a	OREX-800070-104	SEM FIB
2b	OREX-800070-104	TEM FIB
2c	OREX-800070-104	TEM/EDX FIB collection
2d	OREX-800070-104	TEM/FIB collection
2e	OREX-800070-104	TEM FIB
2f	OREX-800070-104	TEM FIB
2g	OREX-800070-104	TEM/EDX FIB collection

93	*2h*	OREX-800070-104	TEM/FIB collection
94			
	3a	OREX-803079-100	TEM FIB
	3b	OREX-803079-100	TEM FIB
	3c	OREX-803079-100	TEM/EDX FIB
	3d	OREX-803079-100	TEM/EDX FIB
	4a	OREX-803079-101	TEM FIB
	4b	OREX-803079-101	TEM FIB
	4c	OREX-803079-101	TEM FIB
	4d	OREX-803079-101	TEM/EDX FIB
	Supplementary Data Video		
	1	OREX-803079-241	XCT reconstruction
	2	OREX-803079-241	XCT reconstruction
	3	OREX-803417-103	XCT reconstruction
	Supplementary Data 1		
	Figure	OREX-803079-241	SEM

Supplementary Data Video 1

Reconstructed three-dimensional model of Bennu particle OREX-803079-241 (left view) from individual XCT tomograms (right views) that correspond to the location of the plane as it transects the particle. The location of a centrally located barred chondrule fragment is highlighted. As the particle matrix becomes translucent, locations of internal (false-colored) chondrule fragments are shown. The highlighted barred chondrule fragment is false-colored orange, and subsequently magnified and oriented to reveal that it is composed of semi-parallel, elongated bars. A total of 35 internal chondrule fragments were identified within this particle.

Supplementary Data Video 2

Reconstructed XCT view of the centrally located barred olivine pyroxene chondrule fragment (false-colored orange) in Bennu particle OREX-803079-241 (see Supplementary Data Video 1). After XCT imaging, this particle was polished to reveal this internal chondrule fragment (see Fig. 4).

Supplementary Data Video 3

Reconstructed three-dimensional model of Bennu particle OREX-803417-103 (left view) from individual XCT tomograms (right views) that correspond to the location of the plane as it transects the particle. As the matrix is removed, chondrule fragments (false-colored green) become visible. One of the fragments breaching the particle surface is highlighted, magnified and oriented to reveal a texture composed of semi-parallel, elongated plates. The location of this chondrule fragment, which breaches the particle surface, is shown in Fig. 5a-c.